# Fuzzy-proportional-integral-derivative-based controller for object tracking in mobile robots

**Duc-Phuc Vuong[1], Trong-Thang Nguyen[2]**
[1]Faculty of Electrical and Electronic Engineering, Vietnam Maritime University, Haiphong, Vietnam
[2]Faculty of Electrical and Electronic Engineering, Thuyloi University, Hanoi, Vietnam

| Article Info | ABSTRACT |
|---|---|
| | This paper aims at designing and implementing an intelligent controller for the orientation control of a two-wheeled mobile robot. The controller is designed in LabVIEW and based on analyzed image parameters from cameras. The image program calculates the distance and angle from the camera to the object. The fuzzy controller will get these parameters as crisp input data and send the calculated velocity as crisp output data to the right and left wheel motor for the robot tracking the target object. The results show that the controller gives a fast response and high reliability and quickly carries out data recovery from system faults. The system also works well in the uncertainties of process variables and without mathematical modeling. |
| | |
| | |

*Corresponding Author:*

Trong-Thang Nguyen
Faculty of Electrical and Electronic Engineering, Thuyloi University
175 Tay Son, Dong Da, Hanoi, Vietnam
Email: nguyentrongthang@tlu.edu.vn

## 1. INTRODUCTION

The robots have been designed to help people in life and improve the efficiency and the quality of production [1], [2]. Several typical works that the robot does very well, such as painting, material handling, manufacturing, and transportation. Today, robots have a more critical role in human life and production. Due to engineering development, mobile robots are more widely applied in human life. One of the most important missions of the mobile robot is following the object.

The position control and orientation control of robots have been proposed by many researchers. However, the algorithms and equations are complicated [3]–[5]. In this research, the authors will use LabVIEW with the IMAQ vision toolbox and fuzzy toolbox [6] to create an orientation control based on the fuzzy logic theory that will facilitate these processes.

The proportional integral derivative (PID) is the most common controller for the robot because of the simple algorithm and high robustness, but low adaptability [7]–[9]. Each controller is only fit for some status and specific subject. Other controllers have been designed for achieving the parameters that are optimal global such as particle swarm optimization and genetic algorithm. However, the defect is decreasing the dynamic qualities and decreasing noise compensation efficiency. The sliding mode controller is a method with a fast response [10]–[12], but there are high-order harmonics. Recently, research [13] defines the optimal values based on the direction of the current track in the established reference frame which is the method based on the improved model predictive current control. The result is that the harmonics are reduced effectively. The grey wolf optimization algorithm-based feedback controller is proposed in the research [14]. The computational efficiency is improved and overshoot is suppressed. The research [15] combines the

model predictive control (MPC) with a sliding-mode disturbance observer. It has improved the accuracy of the current reference and reduced the complexity of the calculation of the observed value for the nonlinear model. Moreover, there are some intelligent controllers such as neural-network-based control [16], [17], fuzzy logic control [18], [19]. These methods can control fast the difficult object.

To take advantage of the different controllers such as the PID controller having high robustness and the fuzzy logic controller having high adaptability, we proposed a combination of the PID controller and fuzzy. The combination of the PID conventional control with fuzzy control [20]–[22] to become a PID-fuzzy controller. Using this controller, the robot will track and follow the object in the various complex environments that previous controllers are very difficult to settle. The proposed block diagram of a controller is shown in Figure 1. By using image processing, the distance (d) and angle from the robot to the camera are calculated, which are the input signals of the controller. The output signals control the velocity of the wheel motors (both left and right wheel motors) to keep the robot going straight to the object. How to create a PID controller is presented in many research so this research only focuses on creating a fuzzy logic controller (FLC) and the experimental study that controls the robot automatically tracking a tennis ball.
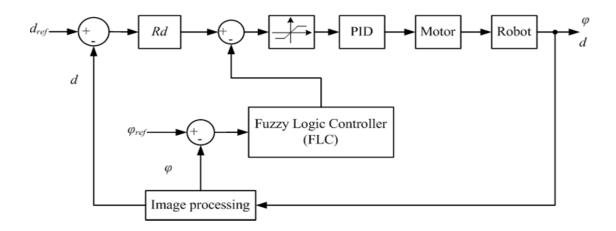


Figure 1. The diagram of the PID-fuzzy controller

## 2.     CALCULATING THE ANGLE AND DISTANCE FROM THE ROBOT TO THE OBJECT

There were many documents showing how to create VIs in LabVIEW to calculate distance as well as the orientation of the camera to the objects. The most common approaches are stereo vision, laser triangulation, optical coherence tomography, and time of flight sensor. To calculate the depth by stereo vision, we use two exact cameras A and B mounted with different perspectives of the subject which is in the P position, and we use the calibration techniques to align pixel information between the extracted depth information and cameras. Ideally, the two cameras are mounted almost parallel to one another and separated by a short distance. Figure 2 shows the diagram of a simplified stereo vision setup, both cameras have the same focal length and are mounted perfectly parallel to each other (variables are described in Table 1). C is the midpoint of AB (CA=CB). When images are acquired from cameras A and B, dR and dL can be calculated exactly, d0 and f are given earlier.

### 2.1.  Calculating angle (φ)

From Figure 2, we have (1).

$$\begin{cases} \tan(\varphi_A) = \frac{d_L}{f} \\ \tan(\varphi_B) = \frac{d_R}{f} \end{cases} \tag{1}$$

Mean that:

$$\begin{cases} CM = \frac{AC}{\tan(\varphi_A)} \\ CN = \frac{BC}{\tan(\varphi_B)} \end{cases} \tag{2}$$

Calculating MN.

$$MN = CN - CM = \frac{BC}{\tan(\varphi_B)} - \frac{AC}{\tan(\varphi_A)} = AC\left(\frac{1}{\tan(\varphi_B)} - \frac{1}{\tan(\varphi_A)}\right) \tag{3}$$

From Figure 2, we also have (4) and (5).

$$\tan(\varphi) = \frac{ML}{CM} = \frac{1}{2}.\frac{MK}{CM} = \frac{1}{2}.\frac{MN.\tan(\varphi_B)}{\frac{AC}{\tan(\varphi_A)}} = \frac{1}{2}.\frac{AC.\left(\frac{1}{\tan(\varphi_B)} - \frac{1}{\tan(\varphi_A)}\right).\tan(\varphi_B)}{\frac{AC}{\tan(\varphi_A)}} \tag{4}$$

$$\tan(\varphi) = \frac{1}{2}.(\tan(\varphi_A) - \tan(\varphi_B)) = \frac{1}{2}.\left(\frac{d_L}{f} - \frac{d_R}{f}\right) \tag{5}$$

Finally, we have (6).

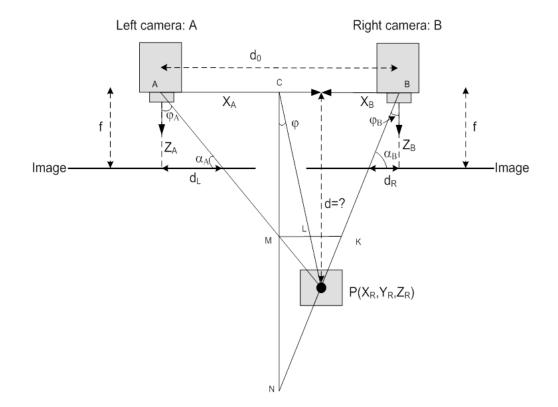$$\varphi = \arctan\left(\frac{1}{2}.\left(\frac{d_L}{f} - \frac{d_R}{f}\right)\right) \tag{6}$$



Figure 2. The simplified vision system

## 2.2. Calculating the distance (d)

From Figure 2, we have (7).

$$\begin{cases} d_L = f.\tan(\varphi_A) = f.\frac{X_A}{d} \\ d_R = f.\tan(\varphi_B) = f.\frac{X_B}{d} = f.\frac{|d_0 - X_A|}{d} \end{cases} \tag{7}$$

So, we have (8) and (9).

$$|d_L - d_R| = f.\frac{d_0}{d} \tag{8}$$

$$d = f \cdot \frac{d_0}{|d_L - d_R|} \tag{9}$$

However, defining the objects such as balls, distance, and angle from camera to object, can be calculated more easily by using only one camera. The following steps are carried out to determine: i) acquiring an image and finding the ball on it; ii) calculating the area in pixels of the ball in that image; iii) calculating the distance to the ball as the following equations. From Figure 3, we have (10).

$$\frac{d'}{d_{ball}} = \frac{f}{d} \tag{10}$$

So, we have (11):

$$d = f \frac{d_{ball}}{d'} = f \cdot \frac{\sqrt{\frac{S_{ball}}{\pi}}}{\sqrt{\frac{4 S_{image}}{\pi}}} = f \cdot \frac{\sqrt{S_{ball}}}{\sqrt{S_{image}}} = \frac{k}{\sqrt{S_{image}}} \tag{11}$$

where $k = f \sqrt{S_{ball}}$ is constant; iv) find out the coordinates of the centroid of the ball acquired on an image having a fixed resolution; and v) determining the angle $\varphi$ from $f$ and $O'B'(O'B')$ that is the difference in pixels between the centroid coordinates and vertical centerline of an image with fixed resolution.

$$\tan(\varphi) = \frac{OB}{d} = \frac{O'B'}{f} \tag{12}$$

$$\varphi = \arctan(\frac{O'B'}{f}) \tag{13}$$
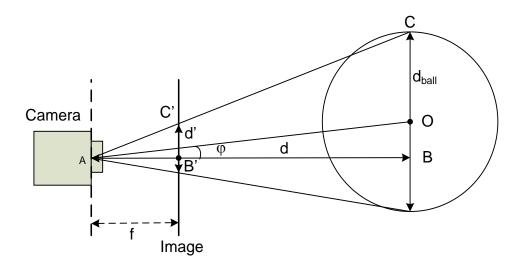
Where all variables are described in Table 1.



Figure 3. Distance and angle from a camera to a ball

Table 1. List of variables

| Symbol | Description | Unit |
|---|---|---|
| d | The distance to the object (depth) | cm |
| $di = AB'$ | The diameter of the projection of the real ball in an image acquired by a camera | cm |
| $d_{ball}$ | The diameter of a real ball | cm |
| $d_{ref}$ | The reference distance from the camera to the ball | cm |
| f | The focal length of a camera | mm |
| $R_d$ | The transfer function of distance control | |
| $S_{ball}$ | The area of the real ball | Pixels |
| $S_{image}$ | The area of the ball in an image acquired by the camera | Pixels |
| d | The distance to the object (depth) | cm |

# 3.    DESIGNING THE FUZZY LOGIC CONTROLLER (FLC)
## 3.1.  Designing the linguistic variables
        The input and output linguistic variables are shown in Figure 4. The inputs are the orientation of the robot ($\Delta\varphi$) and the derivative of orientation (The ROD: $d\Delta\varphi/dt$) reading from the image processing part with the linguistic terms negative big (NB), negative medium (NM), negative small (NS), zero (Z), positive small (PS), positive medium (PM), positive big (PB). Depending on the membership functions for the linguistic terms, their values might correspond to one or more of the linguistic terms.

        Figure 5 shows the input linguistic variables of $\Delta\varphi$ (created in LabVIEW). The range from -70 to 70 specifies that the camera integrated into the robot can detect pattern objects with a range from -70° to +70°. The input linguistic variables of ROD are created as same as the input linguistic variables of $\Delta\varphi$.

        There are two linguistic output variables named Adjustment for the right wheel ($V_{ar}$) and adjustment for the left wheel ($V_{al}$) with the same terms: negative fast (NF), negative medium (NM), negative small (NS), No change (No), positive small (PS), positive medium (PM), positive fast (PF). Figure 6 shows the output linguistic variables of Adjustment for the left wheel created in LabVIEW. The range from -0.35 to 0.35 specifies the adjusted values to output from the PID controller. For output linguistic variables of adjustment for the right wheel are created similarly with range from -0.35 to 0.35.
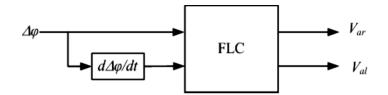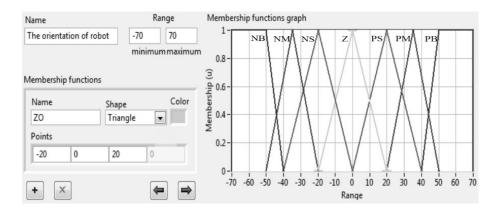


Figure 4. Linguistic variables of FLC
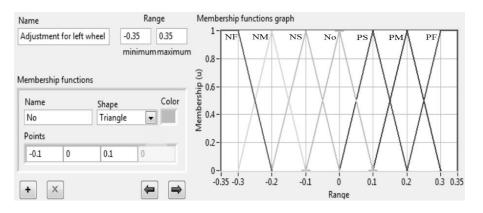


Figure 5. Input linguistic variables of $\Delta\varphi$



Figure 6. Input linguistic variables of adjustment for the left wheel

## 3.2. Designing the rules

The rules describe the relationships between two input linguistic variables and two output linguistic variables. The fuzzy rules are a series of IF-THEN statements that are usually derived from an expert to achieve optimum results [23]–[25]. By experience and practicing the rules for input linguistic variables are described in Tables 2 and 3. The defuzzification method is a center of area.

Table 2. The fuzzy rules of $V_{AR}$

| The ROD | The orientation of the robot | | | | | | |
|---|---|---|---|---|---|---|---|
| | NB | NM | NS | ZO | PS | PM | PB |
| NB | No | PS | PM | PM | PF | PF | PF |
| NM | NS | No | PS | PS | PM | PM | PF |
| NS | NS | NS | No | PS | PS | PM | PM |
| ZO | NM | NS | NS | No | PS | PS | PM |
| PS | NM | NM | NS | NS | No | PS | PS |
| PM | NF | NM | NM | NS | NS | No | PS |
| PB | NF | NF | NF | NM | NM | NS | No |

Table 3. The fuzzy rules of $V_{AL}$

| The ROD | The orientation of the robot | | | | | | |
|---|---|---|---|---|---|---|---|
| | NB | NM | NS | ZO | PS | PM | PB |
| NB | PF | NB | PF | NB | PF | NB | PF |
| NM | PF | PM | PM | PS | PS | No | NS |
| NS | PM | PM | PS | PS | No | NS | NS |
| ZO | PM | PS | PS | No | NS | NS | NM |
| PS | PS | PS | No | NS | NS | NM | NM |
| PM | PS | No | NS | NS | NM | NM | NF |
| PB | No | NS | NM | NM | NF | NF | NF |

## 3.3. Creating the fuzzy controller

We build the control system with a fuzzy controller shown in Figure 7. This is a multiple-input multiple-output (MIMO) type system. The fuzzy controller in FL fuzzy *controller.vi* block is taken from the file named orientation *control.fs*.
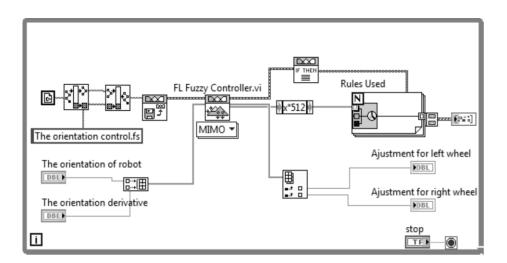


Figure 7. The diagram of the fuzzy controller

## 4. RESULTS AND DISCUSSION
## 4.1. Setting the system

We built the experimental system connection shown in Figure 8. The program was created for the Robot Starter Kit 2.0. The robot integrated an IP camera AXIS M1054 for detecting pattern objects, image acquisition, and processing. This robot will be communicated with a computer by wireless router SWW-5400. The host computer is installed LabVIEW for Robotics Starter Kit software. After developing the robotics VIs, we can download and run the VIs on RT and FPGA targets, such as CompactRIO and single-board RIO products. The host computer also can run VIs that communicates with the VIs running on targets to provide a user interface in which users can control as well as monitor the operation of the robot. In the experimental study, the robot will automatically track a tennis ball based on color as well as distance and angle from the robot to the ball.

## 4.2. Setting the PID controller

The gains, including *P, I,* and *D* are calculated following the Ziegler-Nichols closed-loop tuning method. The optimized values are: *P=0.25, I=0.09, D=0.0117*. The responses of closed-loop systems under PID control are shown in Figure 9. The *X*-axis is time and *Y*-axis is the velocity of the motor in rounds per minute (rpm). Four major characteristics of closed-loop responses are very good. This controller ensures the

low value of settling and the rise times and also has reached the lowest values of the maximum overshoot and steady-state error is almost zero. The PID controller using advanced design algorithms for the DC motor speed control was successfully implemented. It is sufficient to obtain the desired performance in terms of rising time, settling time, overshoot, and steady-state error.
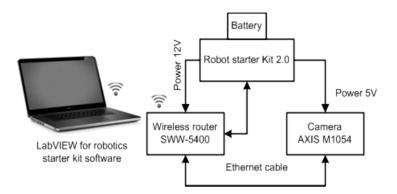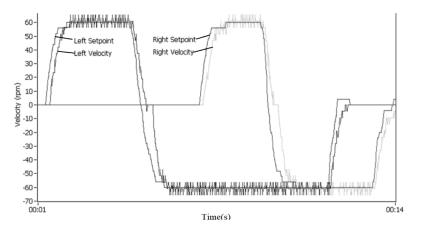


Figure 8. The experimental system connection



Figure 9. Testing with both wheel motors

### 4.3. The accuracy of distance measurement

Testing can be done by comparing the fixed distance of a tennis ball in front of a camera with the indicated values displayed on the screen. The results are shown in Figure 10. It is clear that when the ball appears near the camera (smaller than 60 cm) the difference between the real value and indicator value is very small and the longer the distance the bigger the difference.
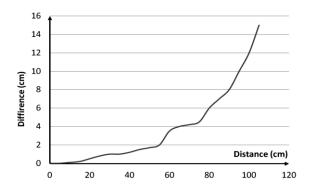


Figure 10. The accuracy of distance measurement

When this IP camera is configured to acquire images at 320×240 resolutions, the system can track the ball in-depth about 100 cm. Over that distance value, the camera cannot detect the ball or receive the results having much difference. To track the ball appearing far from the robot, another specialized camera should be changed.

### 4.4.  The accuracy of angle measurement

It is similar to test distance measurement when the distance is fixed close to 25 cm and the camera is configured to acquire images at 320×240 resolutions. The results are recorded in Figure 11. As seen in Figure 11, the difference between the indicator and real position is very small if the ball appears in the range of the camera. As small as 25 cm in-depth, the camera only detects the ball appearing in front of it with an angle of around $-40^0 \div +40^0$. This range depends on the resolution of a camera and the distance from the camera to the ball. Over this range, the accuracy will decrease even if the camera cannot detect the ball.
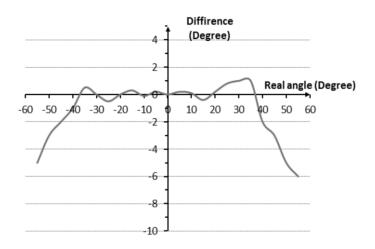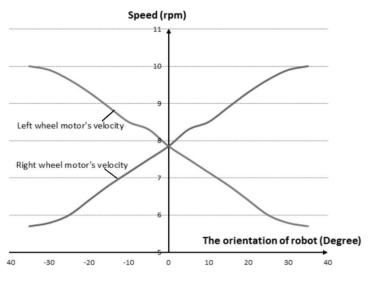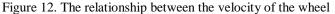
Figure 11. The accuracy of angle measurement

### 4.5.  The controller signals

When the ball moves to the left or the right, the velocity of the motors held left and right wheels changes automatically. These results can be seen in Figure 12. There is an inverse linear relationship between the left wheel motor and the right wheel motor when the orientation of the robot (camera) to the ball is none zero. If the $\Delta\varphi$ is zero velocity of the left wheel motor and the right wheel motor will be the same value (7.8 rpm).

Figure 12. The relationship between the velocity of the wheel

## 4.6. The speed of the robot

Figure 13 shows this relationship when the maximum speed of the robot is fixed at 0.4 m/s and the robot stops when the distance is 10 cm. The speed of a robot depends on the distance. When the PID control is combined with fuzzy logic control, the output from the controller fast responds so that robot tracks the ball quickly and accurately. The quality of the system also depends on light conditions and types of cameras as well as the test environment.
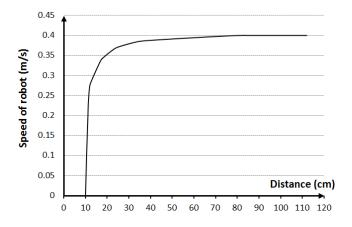


Figure 13. The relationship between the speed of the robot and the distance

## 5.     CONCLUSION

This paper presents the orientation control of a two-wheeled mobile robot using fuzzy logic with LabVIEW by using image processing; an intelligent controller was created without complex modeling of the robot dynamics. The proposed orientation control is the basis for the development of haptic control schemes. The design is also flexible to be straightforward and easily adapted to other types of robots in different domains and for different tasks. It is tested and has satisfactory results in indoor and outdoor environments with a large number of real tennis balls. These contents play an important role in developing and producing service robots that assist mankind in daily life.

## REFERENCES

[1]  S. E. Mathe, A. C. Pamarthy, H. K. Kondaveeti, and S. Vappangi, "A review on raspberry Pi and its robotic applications," in *2022 2nd International Conference on Artificial Intelligence and Signal Processing (AISP)*, Feb. 2022, pp. 1–6, doi: 10.1109/AISP53593.2022.9760590.
[2]  T.-T. Nguyen, "Fractional-order sliding mode controller for the two-link robot arm," *International Journal of Electrical and Computer Engineering (IJECE)*, vol. 10, no. 6, pp. 5579–5585, Dec. 2020, doi: 10.11591/ijece.v10i6.pp5579-5585.
[3]  D. Luo, T. Schauer, M. Roth, and J. Raisch, "Position and orientation control of an omni-directional mobile rehabilitation robot," in *2012 IEEE International Conference on Control Applications*, Oct. 2012, pp. 50–56, doi: 10.1109/CCA.2012.6402680.
[4]  D. Zhao, X. Deng, and J. Yi, "Motion and internal force control for omnidirectional wheeled mobile robots," *IEEE/ASME Transactions on Mechatronics*, vol. 14, no. 3, pp. 382–387, Jun. 2009, doi: 10.1109/TMECH.2009.2018287.
[5]  Y. Liu, J. J. Zhu, R. L. Williams, and J. Wu, "Omni-directional mobile robot controller based on trajectory linearization," *Robotics and Autonomous Systems*, vol. 56, no. 5, pp. 461–479, May 2008, doi: 10.1016/j.robot.2007.08.007.
[6]  NI, *LabVIEW, PID and fuzzy logic toolkit user manual*. Texas: Austin: National Instruments, 2009.
[7]  A. Kherkhar, Y. Chiba, A. Tlemçani, and H. Mamur, "Thermal investigation of a thermoelectric cooler based on Arduino and PID control approach," *Case Studies in Thermal Engineering*, vol. 36, Aug. 2022, doi: 10.1016/j.csite.2022.102249.
[8]  R. P. Borase, D. K. Maghade, S. Y. Sondkar, and S. N. Pawar, "A review of PID control, tuning methods and applications," *International Journal of Dynamics and Control*, vol. 9, no. 2, pp. 818–827, Jun. 2021, doi: 10.1007/s40435-020-00665-4.
[9]  P. B. de Moura Oliveira, "Modern heuristics review for PID control systems optimization: a teaching experiment," in *2005 International Conference on Control and Automation*, 2005, vol. 2, pp. 828–833, doi: 10.1109/ICCA.2005.1528237.
[10] C.-Y. Su and T.-P. Leung, "A sliding mode controller with bound estimation for robot manipulators," *IEEE Transactions on Robotics and Automation*, vol. 9, no. 2, pp. 208–214, Apr. 1993, doi: 10.1109/70.238284.
[11] H. Qin, H. Jing, Z. Hou, Z. Wang, and S. Bai, "Dynamic modeling and sliding mode control of 3-RSS coaxial layout polishing robot," *Journal of the Brazilian Society of Mechanical Sciences and Engineering*, vol. 44, no. 6, Jun. 2022, doi: 10.1007/s40430-022-03509-8.
[12] X. Yang *et al.*, "Continuous friction feedforward sliding mode controller for a trimule hybrid robot," *IEEE/ASME Transactions on Mechatronics*, vol. 23, no. 4, pp. 1673–1683, Aug. 2018, doi: 10.1109/TMECH.2018.2853764.
[13] X. Sun, M. Wu, G. Lei, Y. Guo, and J. Zhu, "An improved model predictive current control for PMSM drives based on current track circle," *IEEE Transactions on Industrial Electronics*, vol. 68, no. 5, pp. 3782–3793, May 2021, doi: 10.1109/TIE.2020.2984433.

[14] X. Sun, C. Hu, G. Lei, Y. Guo, and J. Zhu, "State feedback control for a PM hub motor based on gray wolf optimization algorithm," *IEEE Transactions on Power Electronics*, vol. 35, no. 1, pp. 1136–1146, Jan. 2020, doi: 10.1109/TPEL.2019.2923726.

[15] X. Sun, J. Cao, G. Lei, Y. Guo, and J. Zhu, "A robust deadbeat predictive controller with delay compensation based on composite sliding-mode observer for PMSMs," *IEEE Transactions on Power Electronics*, vol. 36, no. 9, pp. 10742–10752, Sep. 2021, doi: 10.1109/TPEL.2021.3063226.

[16] S. Assahout, H. Elaissaoui, A. El Ougli, B. Tidhaf, and H. Zrouri, "A neural network and fuzzy logic based MPPT algorithm for photovoltaic pumping system," *International Journal of Power Electronics and Drive Systems (IJPEDS)*, vol. 9, no. 4, pp. 1823–1833, Dec. 2018, doi: 10.11591/ijpeds.v9.i4.pp1823-1833.

[17] D. P. Mishra, A. S. Nayak, T. Tripathy, S. R. Salkuti, and S. Mishra, "A novel artificial neural network for power quality improvement in AC microgrid," *International Journal of Power Electronics and Drive Systems (IJPEDS)*, vol. 12, no. 4, pp. 2151–2159, Dec. 2021, doi: 10.11591/ijpeds.v12.i4.pp2151-2159.

[18] C. Dumitrescu, P. Ciotirnae, and C. Vizitiu, "Fuzzy logic for intelligent control system using soft computing applications," *Sensors*, vol. 21, no. 8, Apr. 2021, doi: 10.3390/s21082617.

[19] S. Hosseinpour and A. Martynenko, "Application of fuzzy logic in drying: A review," *Drying Technology*, vol. 40, no. 5, pp. 797–826, Apr. 2022, doi: 10.1080/07373937.2020.1846192.

[20] P. Parikh, S. Sheth, R. Vasani, and J. K. Gohil, "Implementing fuzzy logic controller and PID controller to a DC encoder motor-'A case of an automated guided vehicle,'" *Procedia Manufacturing*, vol. 20, pp. 219–226, 2018, doi: 10.1016/j.promfg.2018.02.032.

[21] A. Kholid, R. A. Fauzi, Y. Y. Nazaruddin, and E. Joelianto, "Power optimization of electric motor using PID-Fuzzy logic controller," in *2019 6th International Conference on Electric Vehicular Technology (ICEVT)*, Nov. 2019, pp. 189–195, doi: 10.1109/ICEVT48285.2019.8993984.

[22] Q.-V. Ngo, C. Yi, and T.-T. Nguyen, "The fuzzy-PID based-pitch angle controller for small-scale wind turbine," *International Journal of Power Electronics and Drive Systems (IJPEDS)*, vol. 11, no. 1, pp. 135–142, Mar. 2020, doi: 10.11591/ijpeds.v11.i1.pp135-142.

[23] M. G. Simões and N. N. Franceschetti, "Fuzzy optimisation-based control of a solar array system," *IEE Proceedings-Electric Power Applications*, vol. 146, no. 5, 1999, doi: 10.1049/ip-epa:19990341.

[24] N. Ouadah, L. Ourak, and F. Boudjema, "Car-like mobile robot oriented positioning by fuzzy controllers," *International Journal of Advanced Robotic Systems*, vol. 5, no. 3, Sep. 2008, doi: 10.5772/5603.

[25] Z. Kovacic and S. Bogdan, *Fuzzy controller design: theory and applications*. CRC Press, 2018.

## BIOGRAPHIES OF AUTHORS

**Duc-Phuc Vuong** received his B.S and M.S degrees in Marine Electrical Engineering and Automation from the Vietnam Maritime University in 2004 and 2007, respectively. He received his Ph.D. degree in Electric and Control Engineering from the Mokpo National Maritime University, Korea, in 2014. He is currently a lecturer at the Department of electric and electronics engineering of Vietnam Maritime University. His research interests are control of industrial machines, Robot control, LabVIEW software, and Recycling energy. He can be contacted at email: phucdtt@gmail.com.

**Trong-Thang Nguyen** received a B.Eng. degree in Automation Control from Hanoi University of Science and Technology in 2005, and a Ph.D. degree in Control Engineering and Automation from the University of Transport and Communications, Vietnam in 2014. He is currently a lecturer in the Control engineering and automation department at Thuyloi University, Vietnam. His research interests include automation control theory, electric drive control, and power generation systems on ships. He can be contacted at email: nguyentrongthang@tlu.edu.vn.